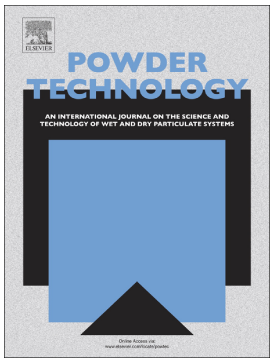

A new method for assessing powder flowability based on physical properties and cohesiveness of particles using a small quantity of samples

Vivek Garg, Tong Deng, Michael S.A. Bradley

PII: S0032-5910(21)00908-6

DOI: https://doi.org/10.1016/j.powtec.2021.10.027

Reference: PTEC 16919

To appear in: *Powder Technology*

Received date: 21 June 2021

Revised date: 15 October 2021

Accepted date: 16 October 2021

Please cite this article as: V. Garg, T. Deng and M.S.A. Bradley, A new method for assessing powder flowability based on physical properties and cohesiveness of particles using a small quantity of samples, *Powder Technology* (2021), https://doi.org/10.1016/j.powtec.2021.10.027

A New Method for Assessing Powder Flowability Based on Physical Properties and Cohesiveness of Particles Using a Small Quantity of Samples

Vivek Garg, Tong Deng* t.deng@gre.ac.uk and Michael SA Bradley

Wolfson Centre for Bulk Solids Handling Technology, Faculty of Engineering & Science, University of Greenwich, Central Avenue, Chatham ME4 4TB, UK

*Corresponding author.

Abstract

Characterising powder flowability can be a challenge if only a small quantity of samples is available, e.g. pharmaceutical formulations. The paper focuses on a new method for assessing powder flowability based on physical properties and cohesiveness of particles using a few grams of powders. The technique applies Bond number to represent powder cohesiveness, which detects particle adhesion at median particle size using a mechanical surface energy tester developed at the Wolfson Centre. To establish the method, correlations between the Bond numbers and the flow functions of several powders measured on a shear cell tester have been explored empirically. With the correlations, a prediction model has been developed not only for powder flow functions but also for other flow properties such as compressibility, internal friction angles and true friction angles. This investigation has been undertaken using a wide range of materials from free-flowing to very cohesive for the method establishment and a group of different types of materials for a blind validation of the method. The methodology shows promising results for powder flowability prediction and other flow properties such as compressibility and internal friction

angles. The validation results show a good agreement against the results measured using a shear cell tester.

Keywords

Powder flowability, Particle properties, Bond number, Cohesive powders, Prediction model

1 Introduction

Powder flowability is an important material property in many powder-formed manufacturing industries for quality control of final products [1]. Especially in pharmaceutical industries, powder flowability is crucial in keeping content uniformity of active pharmaceutical ingredients (API) blended with excipients [2]. Any flow issues can result in severe problems in many processes and substantial financial losses [3]. However, powder flowability is complex and commonly assessed experimentally using a shear cell test [4]. Due to many influential factors involved in various ingredients with different physical properties and selection options in constructing formulations of blends, assessment of powder flowability needs a significant quantity of samples, which is impossible at an early stage in the development of new drugs [5]. Information of material properties for manufacturing purposes are unknown or difficult to measure due to the small quantity of samples available, but it is always a desire to know the flow behaviours of the powders at an early stage. Simply explained, if the powder is too sticky, it will not flow reliably and consistently at the required speed through the production line and give an efficient production rate of acceptable quality. If the powder is too free-flowing, it suffers excessive

segregation and dust emission, consequently causing the uniformity in final products to become poor.

Drug formulators often have many choices in the selection of excipients without considering powder flow issues. However, frequently random selections create serious handling issues for process engineers because of the lack of understanding of material physical properties, including flow behaviour of the materials, and their influences on the process [6]. It is often claimed that there is not enough samples for APIs to have such measurements e.g. flow function tests. APIs are usually a small percentage of the blends but tend to be fine powders, which have more controlling influences over the flow properties of the blends. At an early formulation stage, sample powders of API materials available are often less than grams.

Flowability of a powder is governed by the balance between gravity and particle interactions, chiefly Van der Waals force [7], but the latter is different for every different chemical entity and until now, there has not been a way to measure this effectively. Also, increasingly complex molecules require finer micronisation of API to confer bioavailability, exacerbating the unpredictability of the final blend due to the dominating surface area of the API with unknown van der Waals interaction. For any given manufacturing, there is a "window" of acceptable flow function for the materials. If any formulation of a new drug produces a flow function outside this window, it results in problems in manufacturing. It is important in batch production, but even more critical in continuous manufacturing, where low instantaneous flow rates in handling, small equipment, high process speed to close-coupled requiring compatibility of throughput rates often make the window of acceptable powder

flow properties narrower, and the effects of unpredictable material flowability potentially more catastrophic to profitability.

Various guides suggest that formulators should make an early assessment of the flow behaviour of the powders and proposed blends [8]. However, the existing characterisation tests for flowability all require significant sample powders (from several grams to tens of grams) [9, 10], which creates challenges in assessing powder flowability. Also, at the stage for pre-clinical trials, it is often for a new chemical entity (API, or a mix of APIs to not have the same particle size as the finally micronised materials for adequate bioavailability [11]. Therefore, using available materials to establish flow property tests is meaningless because the change of particle size affects the flow properties significantly.

Using a small sample to predict flowability shows great advantages in solving this challenge because of the less requirement of the sample materials. A new technique has been developed to predict material flowability based on physical properties and cohesiveness of particles measured using a small quantity of powders. With the measurements, a prediction model is established to predict the flow properties not only for single ingredients but also for a complete blend with compensation of particle size effects. The method allows the result to predict the flow function of a powder made from this substance to the formulator's own choice of particle size. It can also be benchmarked against other known blends that are known to be well-behaved or not in the anticipated production equipment, which give an "acceptable window of flow function", to identify any potential problems with the flow of the final blend. This model can then be used to test "what-if" scenarios in terms of changing the size distribution of new APIs or adjusting the excipients to obtain favourable flow properties for manufacturing.

2 Nature of powder flowability

Powder flow is defined as the relative movement of a bulk of particles among neighbouring particles or along a surface of containers [12]. Powder flowability is the ability of granular solids and powders to flow [10]. Flow behaviour of powders is complex and depends on many physical characteristics of the material. In a simple way, powder flowability is the ability of particle movement restricted by material's physical properties that are influenced by environmental conditions and the equipment used for handling, storing, and processing these materials [13]. Because of this, it is hard to fully quantify a powder's flowability by a single test with consideration of all the factors that affect powder flowability including physical properties of powders, humidity, temperature, pressure, and geometry of equipment.

2.1 Bulk properties for powder flow

Flow characteristics of bulk materials can be assessed in many ways including angle of repose, bulk density, angle of internal friction, cohesion, adhesion, and compressibility *etc*. [10]. Commonly, angle of repose, bulk density and friction angles or flow functions are used. An angle of repose is commonly defined as the angle between a horizontal plate and a heap surface of a powder formed by natral discharge onto the horizontal plate [14]. The angle of repose can represent some powder flow properties in nature, such as restriction to flow and powder cohesiveness. However, it limits to no consolidation stress or any compressibility. In most cases of powder flow, consolidation stress is an important factor to influence internal and external frictions [14].

Bulk density of a powder is defined as the mass of powder in a unit volume occupied. The bulk density of a powder may vary significantly depending on many conditions such as

vibration, compaction, consolidation, fluidisation *etc.* [15]. Variation of the bulk density results in a difference in powder flowability. Loose-poured bulk density is formed by random feeding without any vibration, which powders form the powder bed only under the influence of gravity [16]. A powder may have a low loose-poured bulk density if the powder has high internal structural forces (*i.e.* particle-particle or particle-wall bonding), because the forces prevent further collapsing of particles and futher movement of the particles. The high friction between particles limits rearrangement of the powders to utilize the space effectively, and leads to a low bulk density [16]. Therefore, for powder flow, bulk density and compressibility can be indicators for powder flow and important bulk properties for powders.

Friction is a measure of the force required to cause particles to move or slide on each other, which is consequently one of the important properties for powder flow [17]. The internal friction force in systems composed of particles is particle adhesion which is contributed mainly by the Van der Waals force and the liquid bridging force [18]. Cohesion generally increases with a decrease in particle size and with an increase in moisture [19], but particle adhesion could be inversely affected with a increase in particle size and a decrease in moisture [20]. A yield locus plot of failure shear stress versus normal stress for a given consolidating stress is often used for powder flowability indication as flow functions to indicate the flow characteristics of powders [19].

2.2 Common methods for measuring powder flowability

A review of common test methods available for bulk materials can be found in literature [10]. Except for the many bulk flow properties discussed here, *e.g.* angle of repose and bulk density, flow function is the most important property that must be characterised at most of

the time. Generally, shear testers are used to measure the strength to move particles and flow properties of bulk solids at given consolidation stresses [21].

Jenike [22] was the first to establish a fundamental method for characterising the flow of bulk materials and used the principles of plastic failure with the Mohr-Coulomb failure criteria [23]. Ideally, friction is the only reason to resist powder flow in free-flowing powders; but the case becomes more complex in cohesive powders because of compaction and increased mechanical strength in bulk [12]. Several commonly used testers have developed in the past such as Jenike shear cell tester and ring cell shear tester [10]. Mainly the testers produce flow functions for different consolidation stresses (see Fig. 1 as an example) or flowability indices. All these testers have a clear disadvantage that a relatively large amount of sample is required roughly from tens grams to kilograms, depending on the cell size.

Figure 1: Representation of instantaneous flow function of a sample powder.

3 Materials and methods

3.1 Materials

A wide range of powders has been selected for this study, including calcium carbonate, corn starch, plain flour, icing sugar, mannitol, carbamazepine, magnesium stearate, Avicel PH-101, Avicel PH-102, croscarmellose sodium, ibuprofen 70, and bone cement, giving a wide range of material properties and flowability. The calcium carbonate is named with Eskal series grades and manufactured by KSL Staubtechnik GmbH, Germany. The corn starch, plain flour, icing sugar are supplied from local sources, mannitol and magnesium stearate are supplied by Roquette GmbH, Germany. The carbamazepine is from Mylan UK Health Care Limited, UK. Avicel PH-101, Avicel PH-102 are supplied by DuPont Nutrition, Ireland. Ibuprofen 70 is

supplied by BASF, Germany. Bone cement and croscarmellose sodium are provided by a customer of the Wolfson Centre.

3.2 Material characteristics

Characteristics of the materials studied are given in Table 1, where material properties are shown including particle size distibuition as percentile values, size span calculated using the particle size distributions, particle solid density measured using nitrogen pycnometer and Bond numbers measured by a mechanical surface energy tester [20].

Table 1: List of the materials studied and material physical properties

3.2.1 Particle size distributions

The particle size distributions of the powders were measured using the laser diffraction method on a Malvern Mastersizer 2000 (Malvern Instruments, Worcestershire, UK). Particle size span is calculated using Eq. (1) to illustrate the particle size range that will have strong influecnes on powder flow.

$$Span = (d_{90} - d_{10})/d_{50} \quad (1)$$

where, d_{50} represents the size in diameter wher the percentage of powder is less or equal to 50% in volume. d_{10} and d_{90} are the sizes represting 10% and 90% of the powder below the size, respectively.

3.2.2 Scanning Electron Microscopy

Scanning Electron Microscope (SEM) images of poaers show the particle shape and particle agglomerations, which were captured on JSM-5510 Scanning Electron Microscope (make: JEOL Ltd) at the School of Science, University of Greenwich. To take the images, the powders were placed on Aluminium stubs using double-sided carbon tape and coated with a 5-mm

layer of gold/palladium (Au: Pd ¼ 80:20). The instrument was operated at an accelerating voltage of 15 kV and the images were taken at a magnification of 1000. The images of the powders studied can be found in Fig. 2.

Figure 2: SEM images of the materials studied: a) Eskal 2, b) Eskal 4, c) Eskal 10, d) Eskal 15, e) Corn Starch, f) Plain Flour, g) Icing Sugar, h) Mannitol, k), Carbamazepine, m) Magnesium Stearate, n) Avicel PH-101, p) Avicel PH-102, q) Croscarmellose Sodium, s) Ibuprofen 70, t) Bone Cement.

3.3 Methods

3.3.1 Powder flowability

A powder flow tester (PFT) (Brookfield Engineering Laboratories, Inc., Middleboro, MA, USA) was used to determine the flowability of the powders experimentally. The PFT works based on the principles of Jenike's methodology [22] for the determination of the flow function of a powder [24]. It consists of an annular shear cell and a top knifed lid, of which the volume of the cell is 263cc or 43cc for a small trough. Sample powder is generally filled into the cell and the lid is used to apply consolidation stress to the sample. Once a desired consolidation stress level is reached, a shear force is applied to the cell. A torque force generated through the powder to the lid is recorded, which calculates the Mohr circle and the unconfined failure strength at the consolidation stress level.

In this study, flow functions and other flow properties such as compressibility and internal friction angles for the powders were determined with the data obtained. The axial and torsional speeds for the PFT were 1.0 mm/s and 1 rev/hr, respectively. The tests were carried out at ambient temperature (~20-25°C) and humidity (40-60% RH). The equipment was automated with the 'Powder Flow Pro' software and provided the data of yield locus,

flow function curves, trends for wall friction angle versus normal stress, angle of internal friction as a function of major principal consolidating stress. For the current tests, a range of applied uniaxial normal stresses was applied at about 1 to 10 kPa.

3.3.2 Bond number

A cohesive granular Bond number is used for the prediction of powder flowability because of its representative of powder cohesiveness at a median size of the particles [25]. The bond number (B_o) is defined as a ratio of particle adhesion force, F_{ad}, to particle gravity force, F_g, for the particles, as shown in Eq. (2) [26].

$$B_o = F_{ad}/F_g = F_{ad}/mg \quad (2)$$

In this study, a mechanical surface energy tester was used for measuring the Bond numbers given in Table 1 [20]. In the determination of Bond number, a few grammes of commonly available powder (or the same test powders) was compacted to be a substrate disc. If there is not enough sample powder, a standard substrate disc can be used such as glass, TIVAR, mild steel and stainless steel [20]. In the tests, about 50mg of a sample powder was dispersed onto the powder substrate made of the same sample powders using an air expansion disperser operated at a pressure of 1.5 bar. The sampled substrate was weighed to determine the mass of the dispersed sample powder using a digital balance (accuracy of 0.1mg). The substrate disc was fitted onto a carriage that could slide down along a guide under gravity and stop against a buffer to create a measured deceleration to the particles. The mass of the powders detached from the disc was measured by the balance and examined under the Malvern G3 microscope to ascertain the nature and the number of the detached particles and the median size of the particles. The acceleration and the mass (50%

detached from the total dispersed particles) were used for the F_{ad} and the Bond Number in Eq. (2) at the particle size.

4 Results and discussion

Powder flowability of the sample powders has been measured using the PFT tester. With the data, correlations between the flowability and the bond numbers of the powders are explored. Based on the correlations, a prediction model of powder flowability is developed and the model is validated against the data which have not been used for the modelling development.

4.1 Flowability by shear cell tests

As mentioned, shear cell tests are the most popular method for the evaluation of powder flowability. In the current study, 9 sample powders in Table 1 were selected for the modelling development, and the remaining 6 samples were used for modelling validation.

The 9 samples selected covered a wide range of flowability, particle physical properties and cohesiveness, which are believed to have a strong influence on powder flow. The flow functions measure for the samples is shown in Fig. 3., which shows the powders are classified in various flow regimes from free-flowing to nearly very cohesive. In the tests, five consolidation stresses were used for the measurements, which was about 1kPa to 10kPa. With the data, the flow functions of the powders can be obtained by Eq. (3).

$$\boldsymbol{Flow\ Function\ Coefficient}\ (ffc) = \frac{the\ major\ principal\ stress, \sigma_1}{unconfined\ yield\ strength, \sigma_c} \qquad (3)$$

Figure 3: Instantaneous Flow Functions of the 9 sample powders selected.

With results measured using the shear cell tests, others powder properties have been measured and the results are shown in Fig. 4 and 5. In Fig. 4, the results of compressibility, internal friction angles and gradients of failure loci (also called 'true friction angle', defined as the ratio of major consolidation and minor consolidation stresses over the powder element insteady stateflow [22]) are given as a function of unconfined failure strength (σ_c) for a certain consolidation stress level of 1.2 kPa. A general trendline of each variable is added to the graph. For a different level of consolidation stress, the results for the same variables of compressibility, internal friction angles and gradients of failure loci are given in Fig. 5 at a consolidation stress level of 4.8 kPa.

Figure 4: Compressibility, internal friction angles and gradients of failure loci for the 9 sample powders at 1.2 kPa consolidation stress.

Figure 5: Compressibility, internal friction angles and gradients of failure loci for the 9 sample powders at 4.8 kPa consolidation stress.

By the results in Fig. 4 and 5, a common linear trend can be found for the variables, where compressible and internal friction angle are generally increased with an increased unconfined failure strength, but the gradient of failure locus decreases at the same time. The results also show that the slopes of the trendlines may depend on the consolidation stress levels, but the intercepts of the trendlines are quite similar. Compared to the results in Fig. 3 and the results in Fig. 4 and 5, the flowability for the tested powders are significantly different, but for an identical consolidation stress level, there could be a linear correlation between the σ_c and other flow properties. Therefore, if the σ_c can be determined experimentally or theoretically, the whole flow properties of the powder can be predicted through the correlations.

4.2 Correlation between flowability and Bond number

The flowability of the 9 sample powders at the consolidation stress levels of 1.2, 2, 4.8 and 9 kPa are determined using the results in Fig. 3 and given in Table 2. The Bond numbers of the sample powders are also provided in the table. Taking the Bond numbers and the flowability (1/*ffc*), the relationships between the variables are shown in Fig. 6.

Table 2: Flow functions of the sample materials and the Bond numbers

By the results in Fig. 6, linear trendlines are fitted to the data for different levels of consolidation stresses based on a simple judgement of 'highly cohesive powder would be hard to flow'. If a linear relationship between the flowability (1/*ffc*) and the Bond number (*Bo*) is taken, the flowability of a powder can be expressed in Eq. (4) because the data in Fig. 6 do not specify any particular materials, but the slope of the linear relationship and the intercepts of the equations are a function of consolidation stress levels (σ_1) as shown in Eq. (5) and (6).

$$1/ffc = m(Bo) + c \quad (4)$$

Where *m* and *c* are a function of the Bond number. To find the *m* and *c* in Eq. (4), the *m* and *c* in Fig. 6 are plotted versus the consolidation stresses applied and the results are shown in Fig. 7. With empirical best fit, the *m* and *c* can be identified as Eq. (5) and (6), which should be universal for any types of powders.

$$m = a_1 ln(\sigma_1) + b_1 \quad (5)$$

$$c = a_2(\sigma_1)^{b_2} \quad (6)$$

Where a_1, a_2 and b_1, b_2 are constant and -0.020, 0.442, 0.117 and -0.073 respectively for the current study. The constants and the forms of *m* and *c* may change and need further investigation to be validated for other powders.

Figure 6: Correlations between the flowability (1/*ffc*) for the 9 sample powders at the consolidation stress of 1.2, 2, 4.8 and 9 kPa.

Figure 7: Best linear fitted parameters, *m* and *c* interpolating between Bond Number and flowability (1/*ffc*) for different consolidation stress levels

Taking the results in Fig. 4 and 5, a common correlation for the compressibility, internal friction angles and gradient of failure locus (true friction angle) can be formed as:

$$\varphi\left(Comp./\varphi_f/\varphi_r\right) = m_\varphi(\sigma_c) + c_\varphi \quad (7)$$

To find the m_φ and c_φ in Eq. (7), the empirical data of the gradients and intercepts in Fig. 4, 5 and Fig. A1, A2 in the appendix, for the consolidation stress of 2 kPa and 9 kPa, are plotted versus the consolidation stresses (σ_c) and the results are shown in Fig. 8. With empirical best-fit parameters in the figure, the model for compressibility, internal friction angles and gradient of failure locus (true friction angle) can be expressed as:

$$Compressibility = (-0.014\sigma_1 + 0.225)(\sigma_c) + 1.052{\sigma_1}^{0.077} \quad (8)$$

$$Internal\ friction\ angle\ (\varphi_f) = (26.86{\sigma_1}^{-1.186})(\sigma_c) + (0.315\sigma_1 + 31.94) \quad (9)$$

$$True\ friction\ angle\ (\varphi_r) = (4.121\ln(\sigma_1) - 10.06)(\sigma_c) + (-0.09\sigma_1 + 35.93) \quad (10)$$

Figure 8: Best linear fitted parameters, *m* and *c* for compressibility, internal friction angles and gradient of failure locus (true friction angle) for different consolidation stress levels.

4.3 Prediction of powder flowability

Based on the equations Eq. (4), (7) and (8), a model for flowability prediction can be expressed as Eq. (11).

$$1/ffc = (-0.02\ln(\sigma_1) + 0.117)(Bo) + 0.442(\sigma_1)^{-0.073} \quad (11)$$

If a Bond number for a powder is determined, the flow function of the powder can be predicted at given consolidation stress, σ_1. Because of flow function (*ffc*) = σ_1/σ_c, the σ_c values can be obtained with a known flowability if a σ_1 is given. Taking the model shown in Eq. (11) and four consolidation stresses at 1.2, 2, 4.8 and 9 kPa, the predicted flow functions for the 9 sample powders are shown in Fig. 9 as lines named by material name plus -p. The experimental measurements for the same powders are also given in the figure, which is marked with the same colour as dots.

Figure 9: Comparison between the flowability prediction based on Bond Numbers and the measurements of the flowability (1/*ffc*) for the 9 sample powders.

Compared to the results in Fig. 9, it shows the model generally works well. However, some materials show over-predicted values, such as Eskal 15, but some materials are under predicted, such as icing sugar, plain flour, and mannitol. For the rest of the materials, including Eskal 4, Eskal 10, corn starch and Carbamazepine, the predictions are well fitted to the experimental data and have a small prediction error. Comparing the results at the consolidation stress of about 9 kPa, for Eskal 15, the model shows about 65% over-predicted, but for mannitol, the model indicates approximately 34% under-predicted. It is noticed that Eskal 15 and mannitol all have a significant error, but the errors would have less effects on the flow properties because they are all classified under the free-flowing region.

Flowability is more critical to the cohesive powders, where the model does work well. For plain flour, the prediction error at 8.0 kPa is about 18% under-estimated. For icing sugar, the error at 9 kPa is about 20% under-estimated. For Eskal 2, the error at 9 kPa is about 10% under-estimated. For Eskal 10, the error at 9 kPa is about 3% under-estimated. For the rest of materials including Eskal 4, corn starch and carbamazepine, the error at 9 kPa is all less than 1%, which the materials are likely cohesive ones.

However, at low consolidation stress levels, the model works better and gives slightly higher accuracy for the predictions for the above materials. It is observed that, for cohesive powders, at the consolidation stress level of 1.25 kPa, the errors between the experiment and the predictions are approximately between 4% to 10%, whereas for coarser materials, the error becomes significant to about 30%. The results clearly show that the predictions from the model have less errors at low consolidation stress compared to high consolidation stresses.

As the correlations are shown in Eq. (8-10), this model can be extended to the prediction of other flow properties such as compressibility, internal friction angle and gradient of failure locus (true friction angle). In the equations, the σ_c is determined by the Eq. (11), and the consolidation stresses given. Therefore, the model can provide a complete assessment for a powder without carrying out a shear cell test. A typical result of comparison between the prediction of compressibility and the measurements is given in Fig. 10 as an example.

Figure 10: Prediction of the compressibility based on the predicted flow function (*ffc*) at given consolidation stress and compression to the measurements for the 9 sample powders.

4.4 Validation of flow function prediction

For the model developed, a blind validation of flow function prediction is taken using the remaining 6 powders in Table1, which has not been used for the model development. The comparison results between the prediction of the flow functions based on the Bond Numbers and the experimental measurements are shown in Fig. 11. The same validation for compressibility is taken for the 6 sample powders. The comparison results are shown in Fig. 12. To show the details, the Y-axis in Fig. 12 is zoomed in.

The data in Fig. 10 and Fig. 12, show that the prediction model has a reasonably good agreement with the results using a shear cell tester. Therefore, the model developed can be used for assessing powder flowability just using material physical properties and Bond number. Because material characterisation and Bond number measurement use a relatively small sample, the model can use only a few grams of samples to give an idea of powder flowability. The model can be used for situations where there are not enough samples available or rapid tests required for many sample powders. Alternatively, the model can be used to benchmark against many possibilities, so a "window of acceptable flow function" can be identified against any potential problems for powder flow. This model also can be used to test "what-if" scenarios for blends in terms of changing the size distribution of new APIs or adjusting the excipients to obtain favourable flow properties for manufacturing.

Figure 11: Validation comparison between the prediction of the flow functions based on the Bond Numbers and the measurements for the 6 sample powders.

Figure 12: Validation comparison between the compressibility predicted by the model and the measurements for the 6 sample powders.

5 Conclusions

In this study, a new method for assessing powder flowability has been developed based on particle physical properties and Bond number using a small quantity of samples. Experimental results show a strong linear correlation between the Bond number and the flow function. The study used 9 sample powders to establish the correlations, and the slope and the intercept for the linear relationship have been identified.

The flowability model developed shows a universal correlation regardless of the sample materials. With the Bond number and the material properties including particle size, the flow function can be determined. The study shows significant errors for free-flowing materials, but better accuracy for cohesive materials where the errors are less than 1%. In general, the model gives a good prediction within an error range. Also, the study shows the model can be extended to other flow properties such as compressibility, internal friction angle and true friction angle. The correlations created empirically also show linear relations and give a good prediction model.

Validations of the model show that the prediction model has a good agreement with the experimental data measured using a PFT tester. The results follow the same trends as the shear cell tester gives. Therefore, the model shows a great advantage, because the model allows assessing powder flowability using a few grams of samples. The prediction model can be used for the situation when enough sample is impossible to obtain at the early stage of formulation development. This will benefit any non-professional users to assess powder flowability or use it as an indication for evaluating the flowability of powders in formulation selection of powders.

Acknowledgement

This work was financially supported by a Vice-Chancellor Scholarship, University of Greenwich, UK and the British Engineering and Physical Sciences Research Council [EPSRC grant number: EP/N025261/1], the Virtual Formulation Laboratory (VFL) for prediction and optimisation of manufacturability of advanced solids. It is also kindly acknowledged for partial funding and providing four of tested materials the EPSRC Future Manufacturing Research Hub in Continuous Manufacturing and Advanced Crystallisation (CMAC, EPSRC grant number: EP/P006965/1) and the Engineering and Physical Sciences Research Council, through the project Feasibility Studies of Advanced Manufacturing Technologies.

References

1. Schulze, D. (2008). Powders and bulk solids. Behaviour, characterization, storage and flow. Springer, 22.
2. Alyami, H., Dahmash, E., Bowen, J., & Mohammed, A. R. (2017). An investigation into the effects of excipient particle size, blending techniques and processing parameters on the homogeneity and content uniformity of a blend containing low-dose model drug. PloS one, 12(6), e0178772.
3. Krantz, M., Zhang, H., & Zhu, J. (2009). Characterisation of powder flow: Static and dynamic testing. Powder Technology, 194(3), 239-245.
4. Salehi, H., Barletta, D., & Poletto, M. (2017). A comparison between powder flow property testers. Particuology, 32, 10-20.
5. Vanarase, A. U., Osorio, J. G., & Muzzio, F. J. (2013). Effects of powder flow properties and shear environment on the performance of continuous mixing of pharmaceutical powders. Powder technology, 246, 63-72
6. Garg, V., Mallick, S. S., García-Trinanes, P., & Berry, R. J. (2018). An investigation into the flowability of fine powders used in pharmaceutical industries. Powder technology, 336, 375-382.

7. Jones, R., Pollock, H. M., Geldart, D., & Verlinden, A. (2003). Inter-particle forces in cohesive powders studied by AFM: effects of relative humidity, particle size and wall adhesion. Powder Technology, 132(2-3), 196-210.
8. Macri, D., Chirone, R., Salehi, H., Sofia, D., Materazzi, M., Barletta, D., ... & Poletto, M. (2020). Characterisation of the Bulk Flow Properties of Industrial Powders from Shear Tests. Processes, 8(5), 540.
9. Hassanpour, A., Hare, C., & Pasha, M. (Eds.). (2019). Powder flow: Theory, characterisation and application. Royal Society of Chemistry
10. Ganesan, V., Rosentrater, K.A., & Muthukumarappan, K. (2008). Flowability and handling characteristics of bulk solids and powders–a review with implications for DDGS. biosystems engineering, 101(4), 425-435.
11. Cun, D., Zhang, C., Bera, H., & Yang, M. (2021). Particle engineering principles and technologies for pharmaceutical biologics. Advanced Drug Delivery Reviews, 174, 140-167.
12. Peleg, M. (1977). Flowability of food powders and methods for its evaluation—a review. Journal of Food Process Engineering, 1(4), 303-328.
13. Prescott, J. K., & Barnum, R. A. (2000). On powder flowability. Pharmaceutical technology, 24(10), 60-85.
14. Al-Hashemi, H. M. B., & Al Amoudi, O. S. B. (2018). A review on the angle of repose of granular materials. Powder technology, 330, 397-417.
15. Rosentrater, K. A., & Muthukumarappan, K. (2006). Corn ethanol coproducts: generation, properties, and future prospects. International Sugar Journal, 108(1295), 648-657.
16. Abdullah, E. C., & Geldart, D. (1999). The use of bulk density measurements as flowability indicators. Powder technology, 102(2), 151-165.
17. Johanson, J. R. (1972). Modeling flow of bulk solids. Powder Technology, 5(2), 93-99.
18. Weber, M. W., Hoffman, D. K., & Hrenya, C. M. (2004). Discrete-particle simulations of cohesive granular flow using a square-well potential. Granular Matter, 6(4), 239-254.

19. Fitzpatrick, J. J., Barringer, S. A., & Iqbal, T. (2004). Flow property measurement of food powders and sensitivity of Jenike's hopper design methodology to the measured values. Journal of Food Engineering, 61(3), 399-405.

20. Deng, T., Garg, V., & Bradley, M. S. (2021). A study of particle adhesion for cohesive powders using a novel mechanical surface energy tester. Powder Technology, 391, 46-56.

21. Schwedes, J. (2002). Consolidation and flow of cohesive bulk solids. Chemical Engineering Science, 57(2), 287-294.

22. Jenike, A. W. (1976). Storage and flow of solids. Bulletin No. 123 of the Utah Engineering Experiment Station; Vol. 53, No. 26, November 1964 (No. NP-22770). Utah Univ., Salt Lake City (United States).

23. Thomson, F. M. (1997). Storage and flow of particulate solids. In Handbook of Powder Science & Technology (pp. 389-486). Springer, Boston, MA, USA.

24. Berry, R. J., Bradley, M. S. A., & McGregor, R. G. (2015). Brookfield powder flow tester–Results of round robin tests with CRM-116 limestone powder. Proceedings of the Institution of Mechanical Engineers, Part E: Journal of Process Mechanical Engineering, 229(3), 215-230.

25. Castellanos, A. (2005). The relationship between attractive interparticle forces and bulk behaviour in dry and uncharged fine powders. Advances in physics, 54(4), 263-376.

26. Capece, M., Ho, R., Strong, J., & Gao, P. (2015). Prediction of powder flow performance using a multi-component granular Bond number. Powder Technology, 286, 561-571.

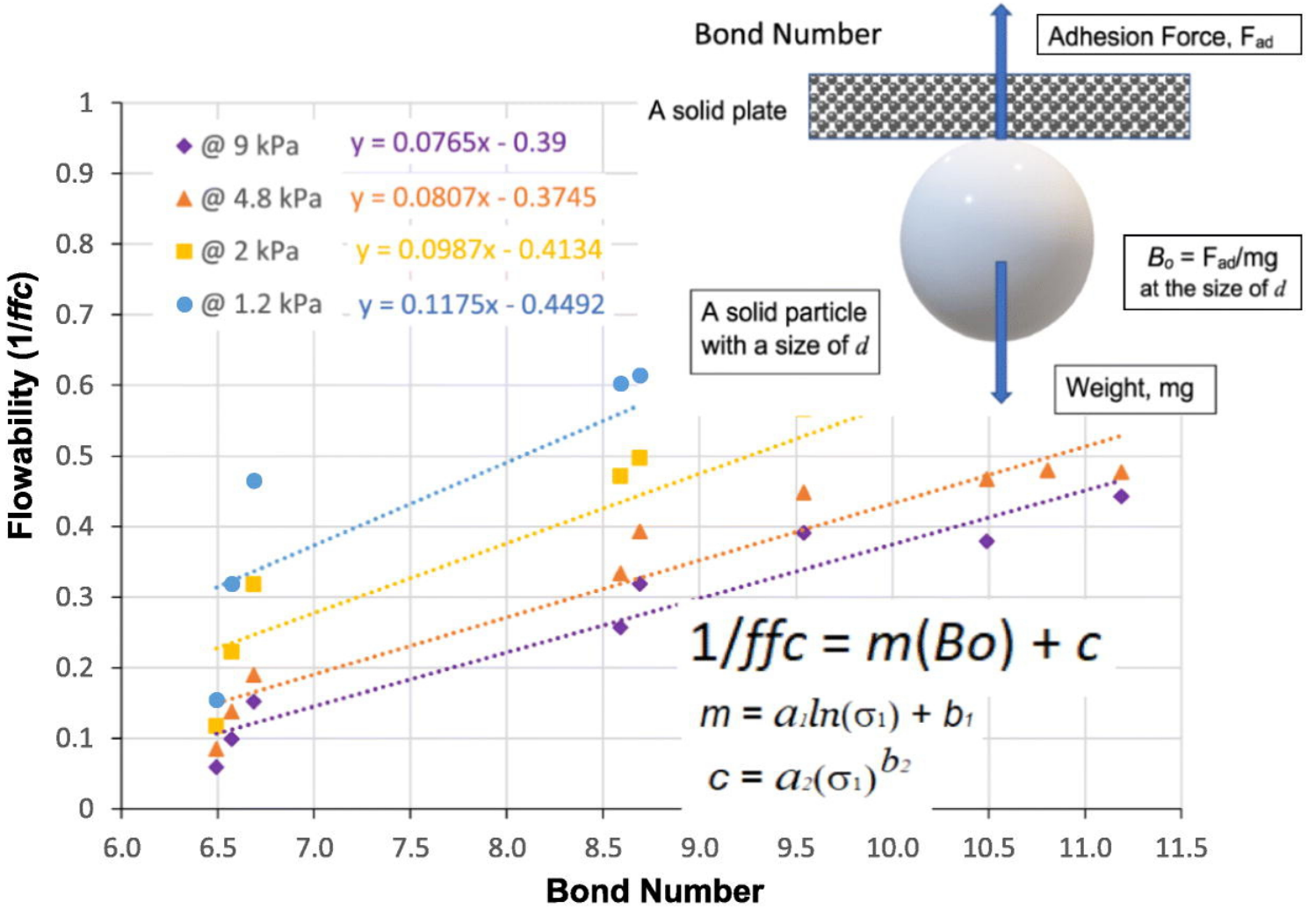

Graphics Abstract

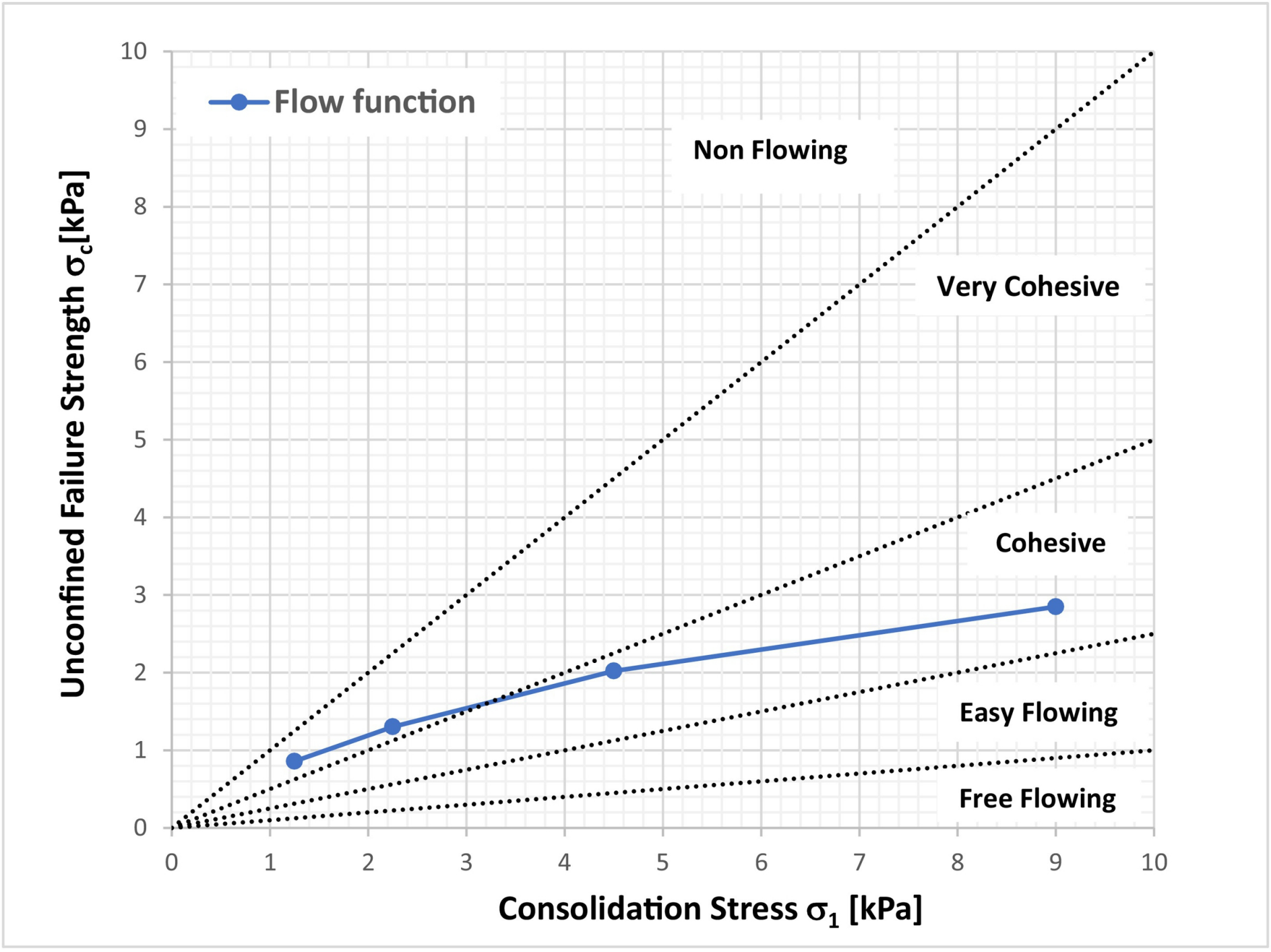
Flow function
Non Flowing
Very Cohesive
Cohesive
Easy Flowing
Free Flowing
Unconfined Failure Strength σc[kPa]
Consolidation Stress σ1 [kPa]
0
1
2
3
4
5
6
7
8
9
10

Figure 1

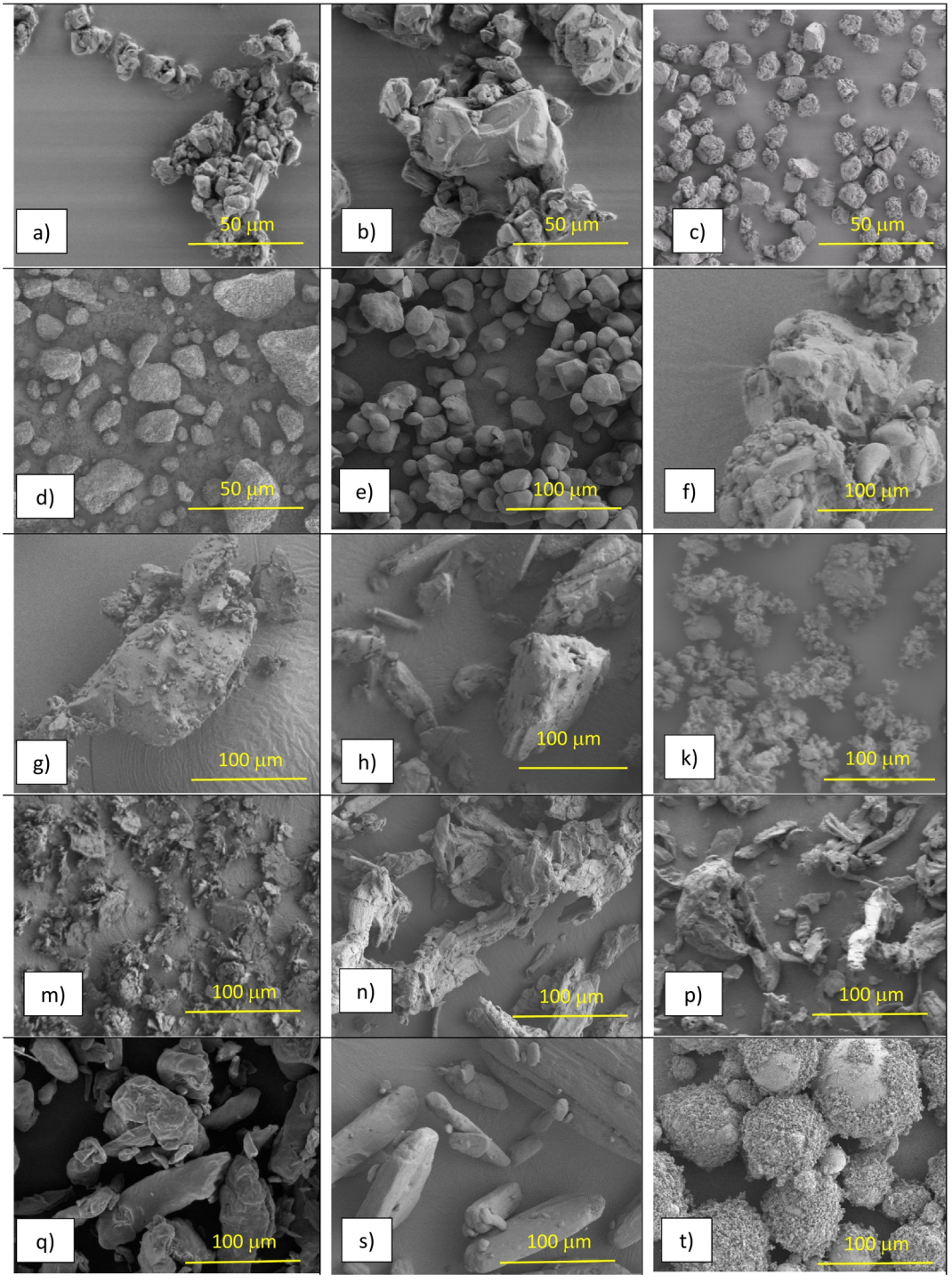
a)
50 µm
b)
50 µm
c)
50 µm
d)
50 µm
e)
100 µm
f)
100 µm
g)
100 µm
h)
100 µm
k)
100 µm
m)
100 µm
n)
100 µm
p)
100 µm
q)
100 µm
s)
100 µm
t)
100 µm

Figure 2

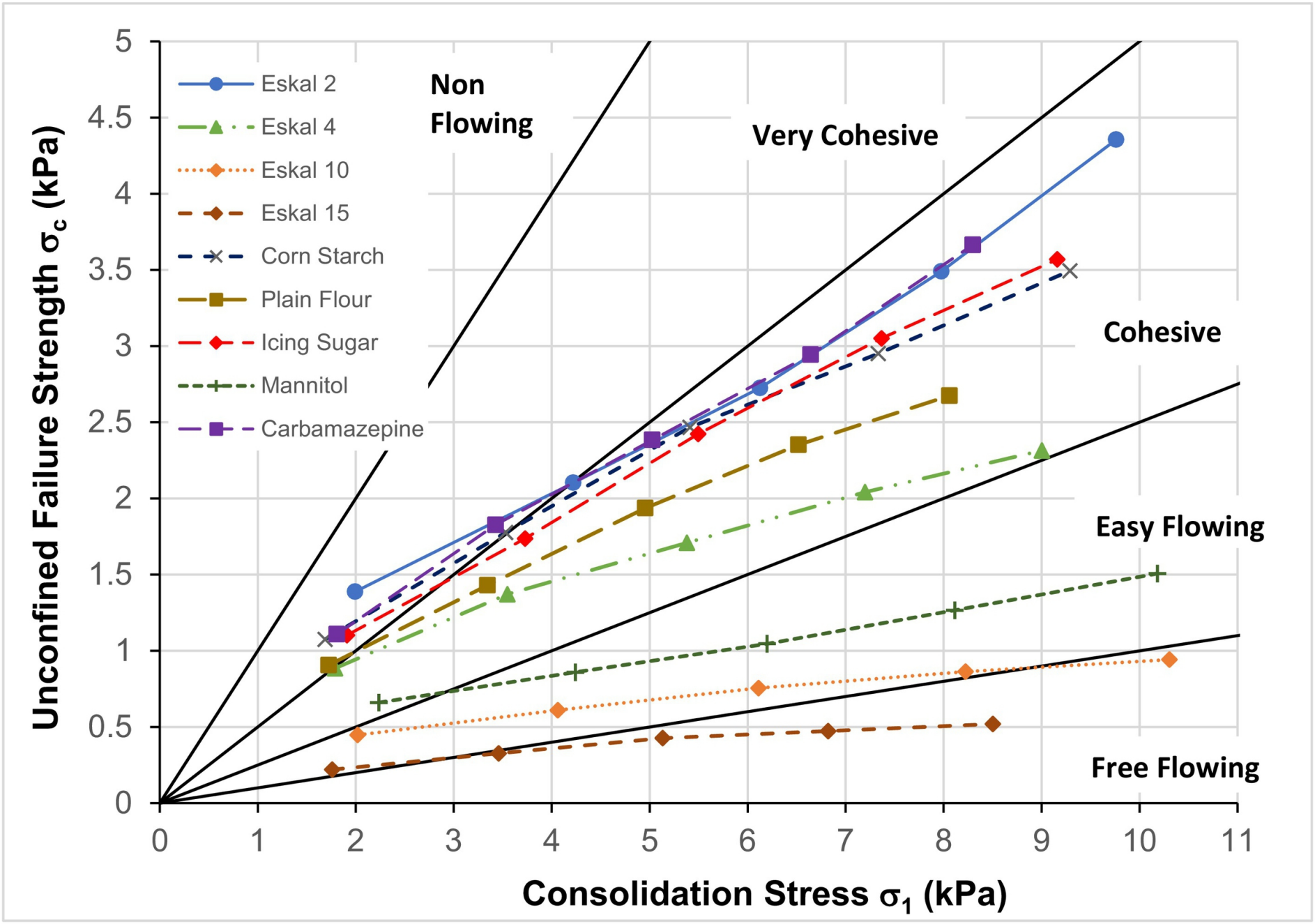
Unconfined Failure Strength σ_c (kPa)
Consolidation Stress σ_1 (kPa)
Eskal 2
Eskal 4
Eskal 10
Eskal 15
Corn Starch
Plain Flour
Icing Sugar
Mannitol
Carbamazepine
Non Flowing
Very Cohesive
Cohesive
Easy Flowing
Free Flowing
0
0.5
1
1.5
2
2.5
3
3.5
4
4.5
5
0
1
2
3
4
5
6
7
8
9
10
11

Figure 3

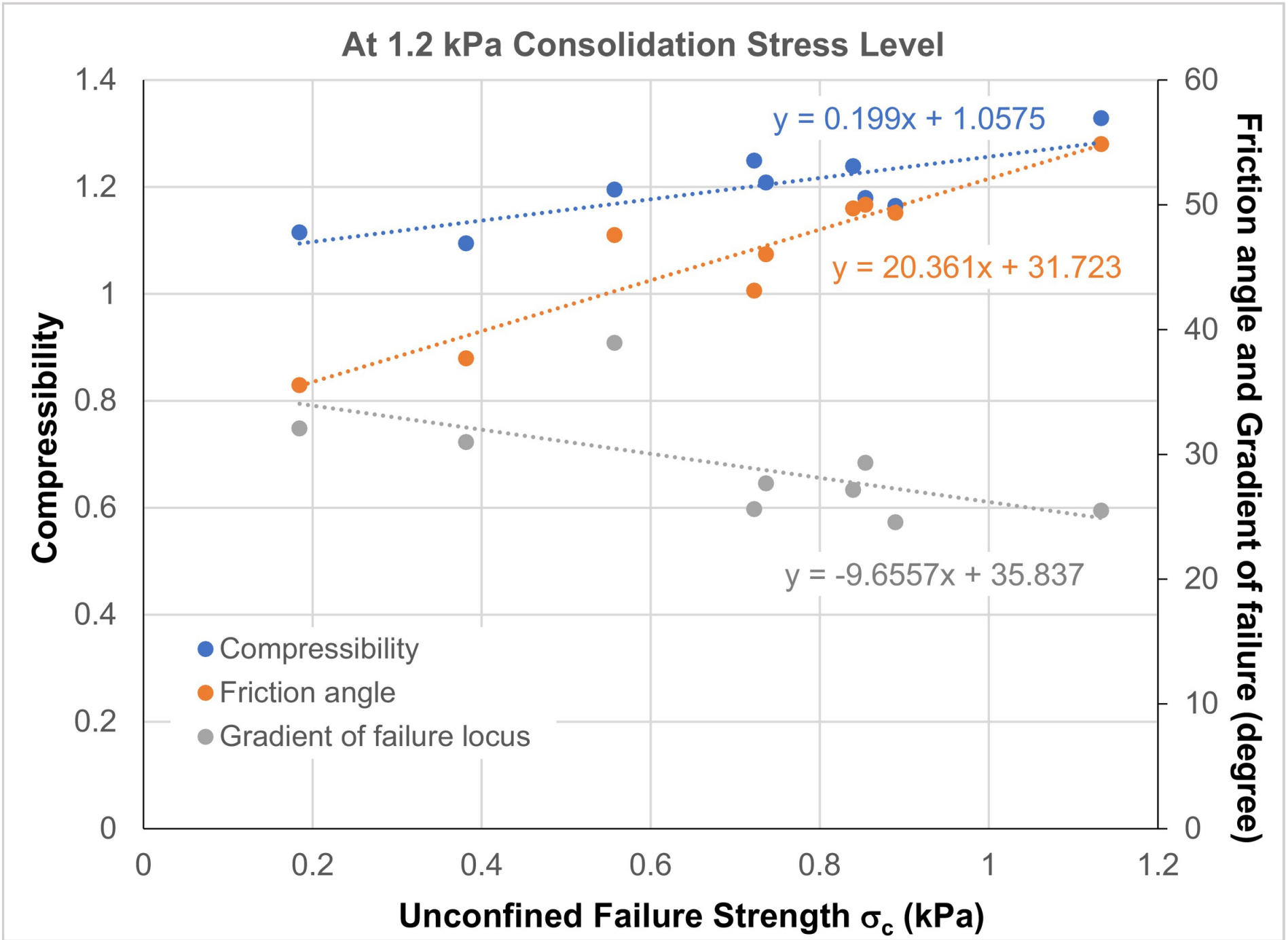
At 1.2 kPa Consolidation Stress Level
y = 0.199x + 1.0575
y = 20.361x + 31.723
y = -9.6557x + 35.837
Compressibility
Friction angle
Gradient of failure locus
Compressibility
Friction angle and Gradient of failure (degree)
Unconfined Failure Strength σc (kPa)
0
0.2
0.4
0.6
0.8
1
1.2
1.4
0
10
20
30
40
50
60

Figure 4

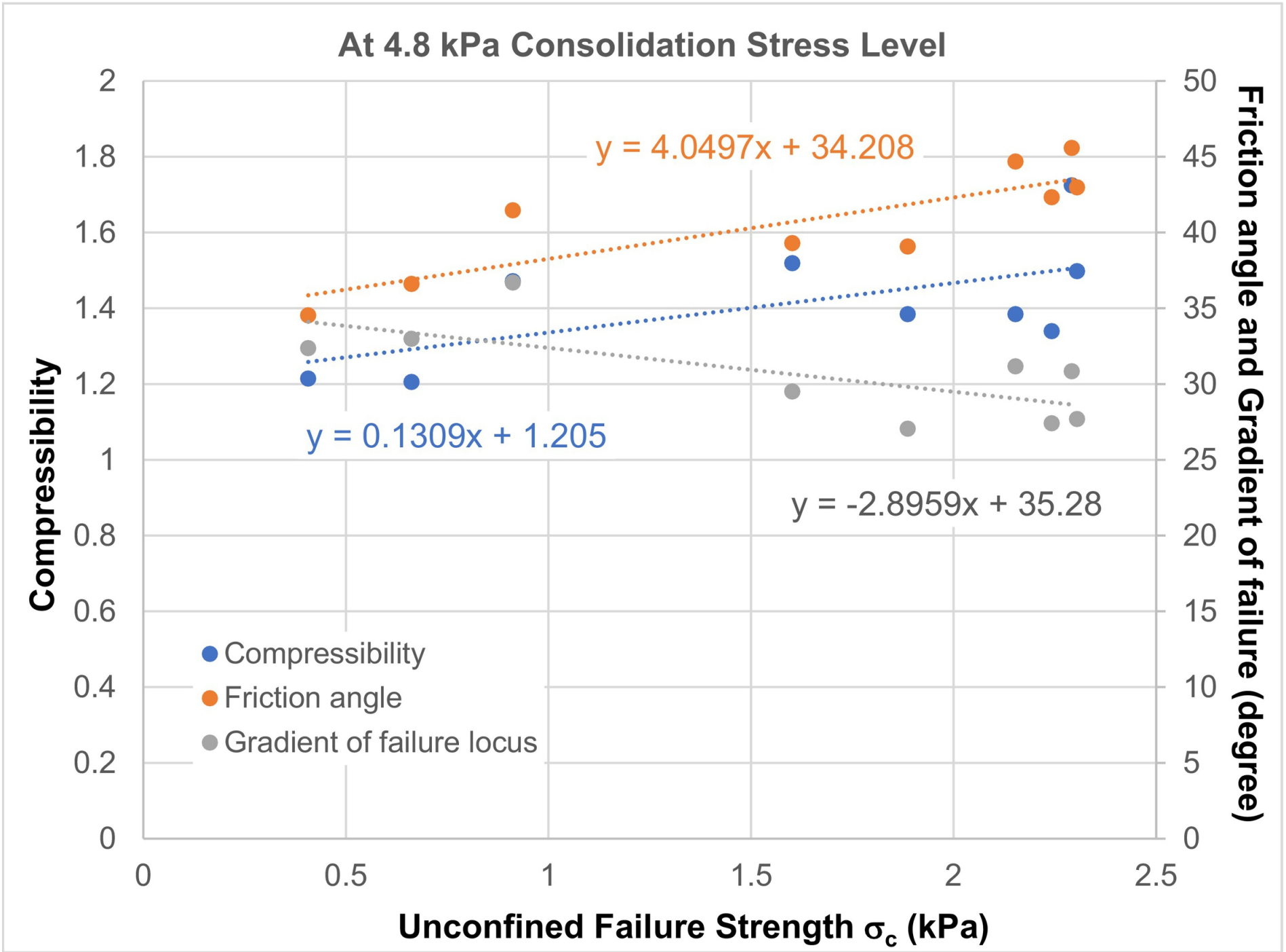
At 4.8 kPa Consolidation Stress Level
y = 4.0497x + 34.208
y = 0.1309x + 1.205
y = -2.8959x + 35.28
Compressibility
Friction angle
Gradient of failure locus
Compressibility
Friction angle and Gradient of failure (degree)
Unconfined Failure Strength σc (kPa)
0
0.2
0.4
0.6
0.8
1
1.2
1.4
1.6
1.8
2
0
5
10
15
20
25
30
35
40
45
50
0
0.5
1
1.5
2
2.5

Figure 5

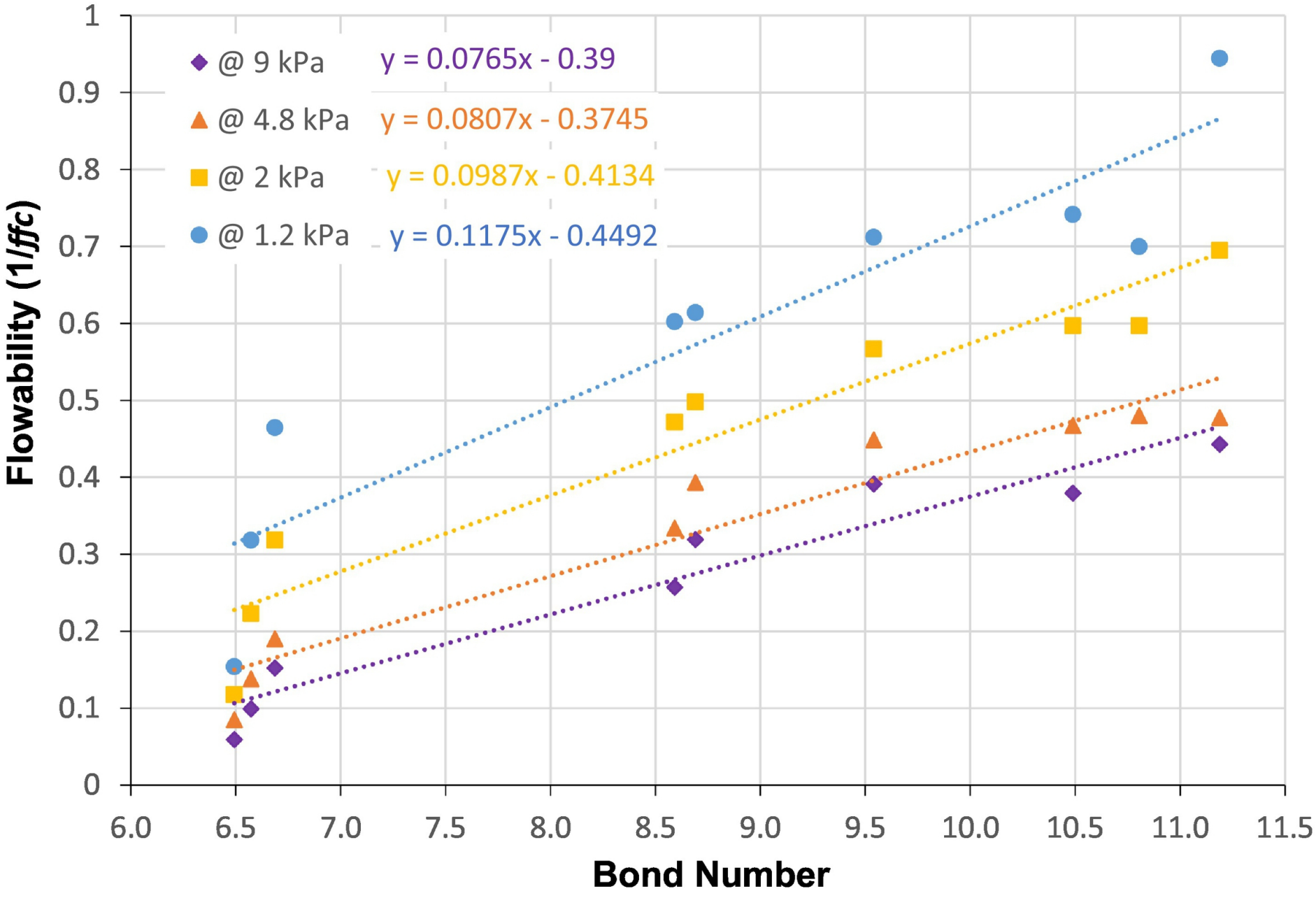
@ 9 kPa
y = 0.0765x - 0.39
@ 4.8 kPa
y = 0.0807x - 0.3745
@ 2 kPa
y = 0.0987x - 0.4134
@ 1.2 kPa
y = 0.1175x - 0.4492
Flowability (1/ffc)
Bond Number
0
0.1
0.2
0.3
0.4
0.5
0.6
0.7
0.8
0.9
1
6.0
6.5
7.0
7.5
8.0
8.5
9.0
9.5
10.0
10.5
11.0
11.5

Figure 6

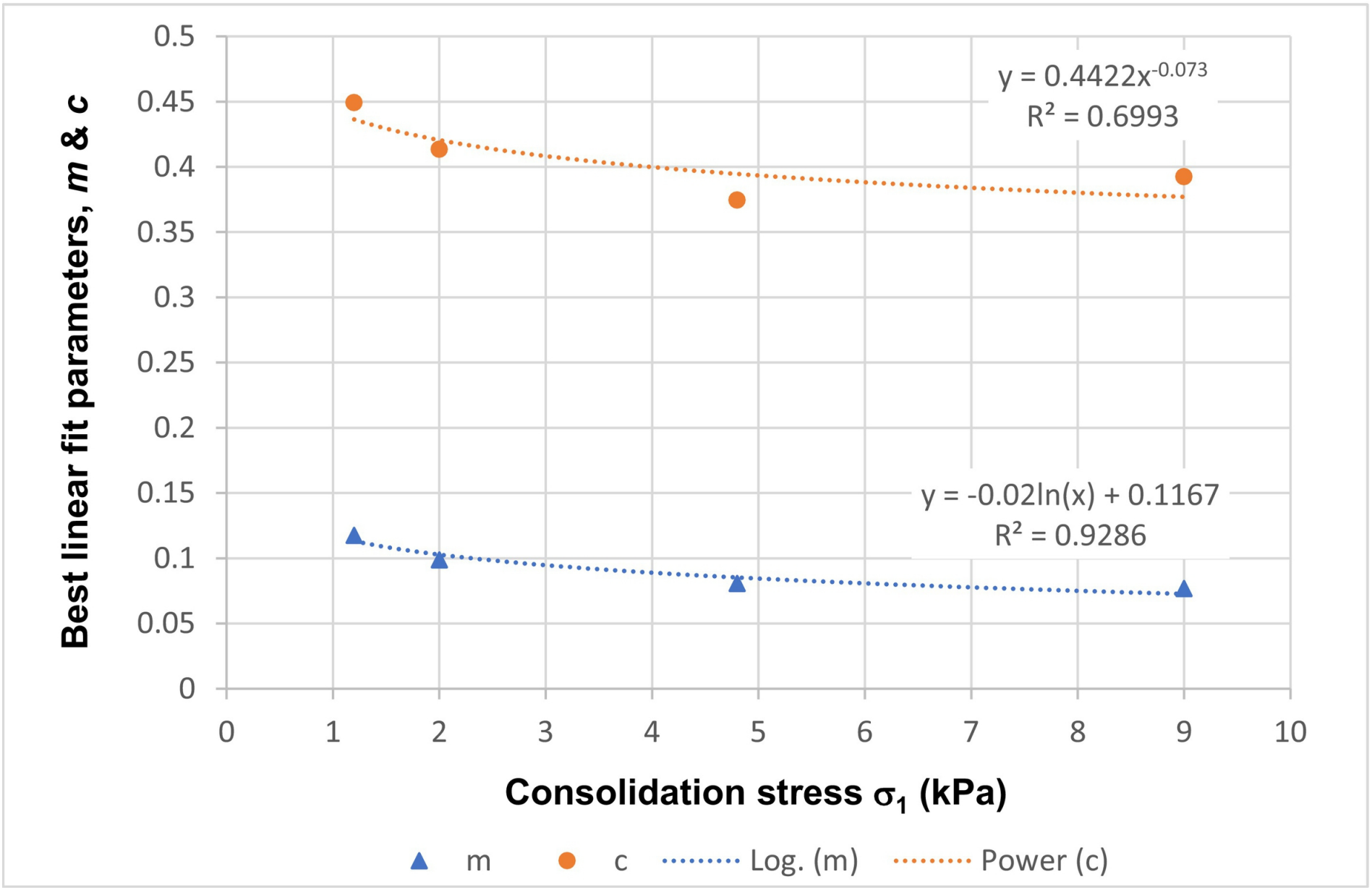
Best linear fit parameters, m & c
0.5
0.45
0.4
0.35
0.3
0.25
0.2
0.15
0.1
0.05
0
y = 0.4422x-0.073
R² = 0.6993
y = -0.02ln(x) + 0.1167
R² = 0.9286
0
1
2
3
4
5
6
7
8
9
10
Consolidation stress σ1 (kPa)
m
c
Log. (m)
Power (c)

Figure 7

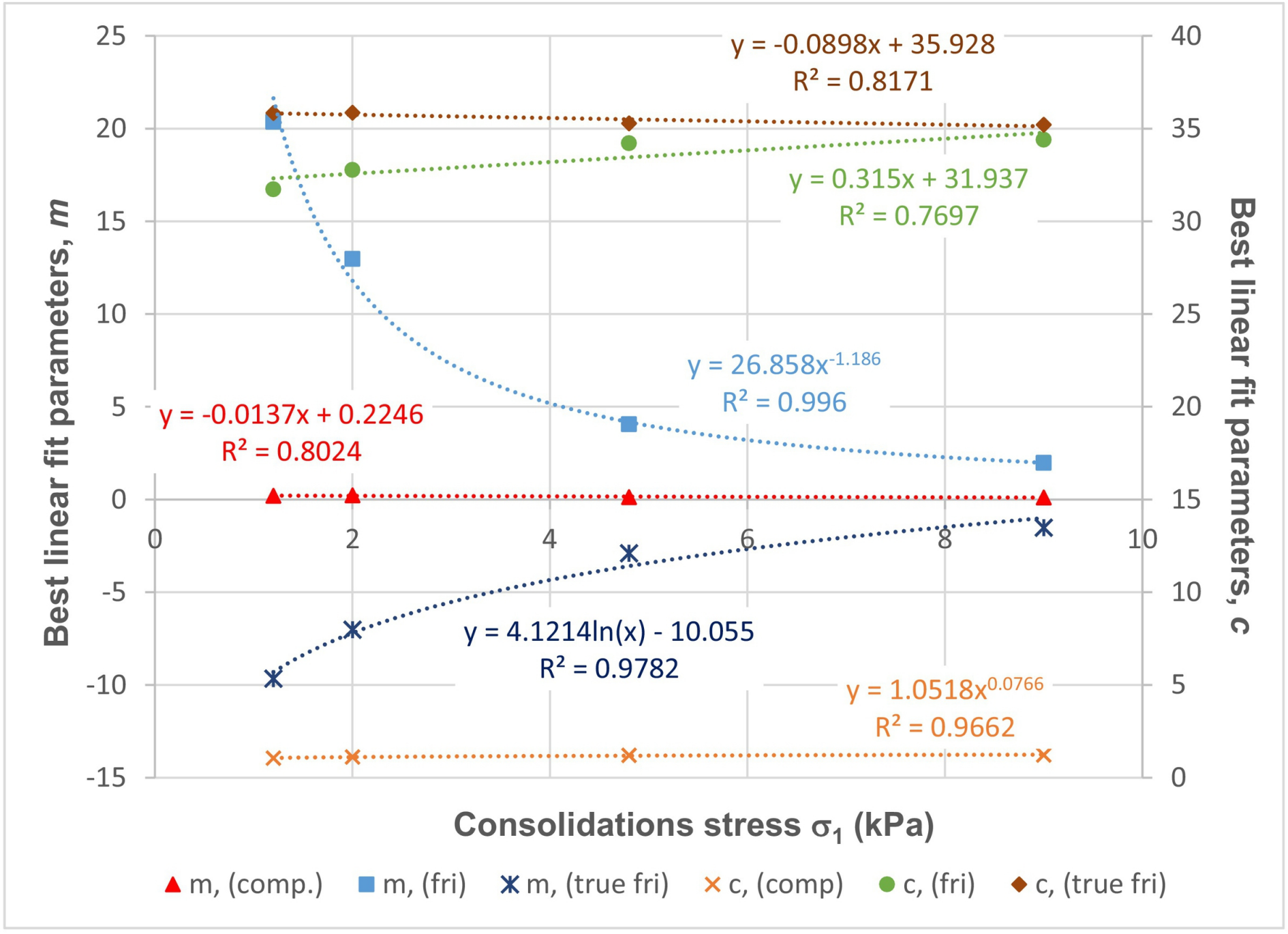
y = -0.0898x + 35.928
R² = 0.8171
y = 0.315x + 31.937
R² = 0.7697
y = 26.858x^-1.186
R² = 0.996
y = -0.0137x + 0.2246
R² = 0.8024
y = 4.1214ln(x) - 10.055
R² = 0.9782
y = 1.0518x^0.0766
R² = 0.9662
Best linear fit parameters, m
Best linear fit parameters, c
Consolidations stress σ1 (kPa)
m, (comp.)
m, (fri)
m, (true fri)
c, (comp)
c, (fri)
c, (true fri)

Figure 8

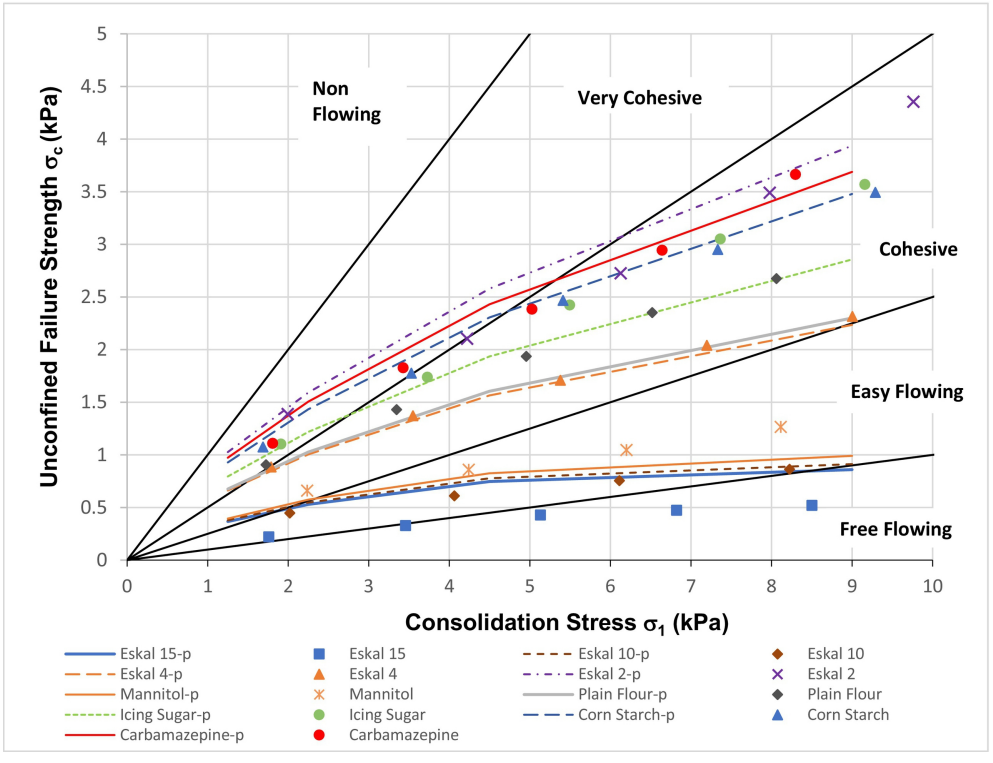
Unconfined Failure Strength σ_c (kPa)
Consolidation Stress σ_1 (kPa)
Non Flowing
Very Cohesive
Cohesive
Easy Flowing
Free Flowing
0
0.5
1
1.5
2
2.5
3
3.5
4
4.5
5
0
1
2
3
4
5
6
7
8
9
10
Eskal 15-p
Eskal 15
Eskal 10-p
Eskal 10
Eskal 4-p
Eskal 4
Eskal 2-p
Eskal 2
Mannitol-p
Mannitol
Plain Flour-p
Plain Flour
Icing Sugar-p
Icing Sugar
Corn Starch-p
Corn Starch
Carbamazepine-p
Carbamazepine

Figure 9

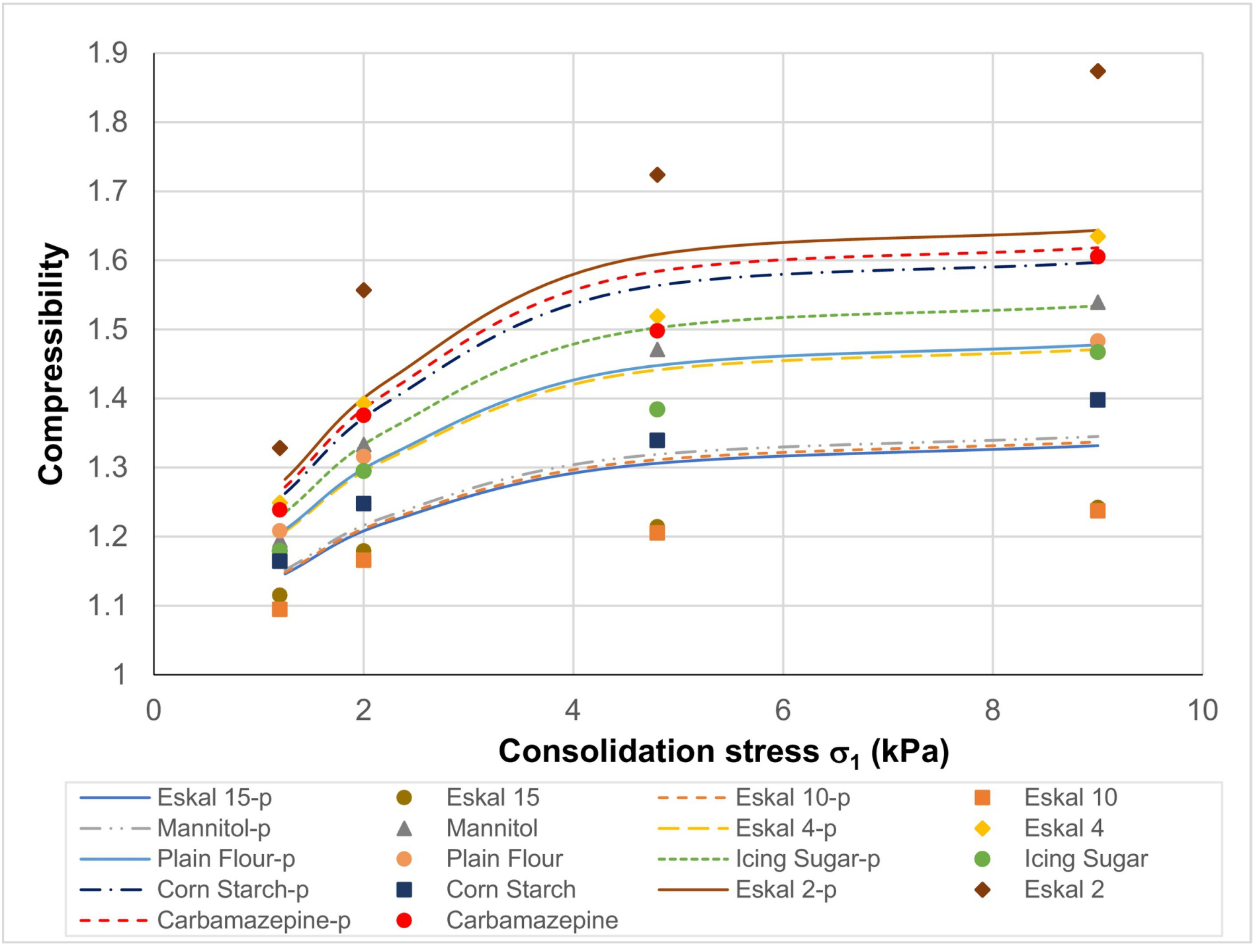
Compressibility
1.9
1.8
1.7
1.6
1.5
1.4
1.3
1.2
1.1
1
0
2
4
6
8
10
Consolidation stress σ1 (kPa)
Eskal 15-p
Eskal 15
Eskal 10-p
Eskal 10
Mannitol-p
Mannitol
Eskal 4-p
Eskal 4
Plain Flour-p
Plain Flour
Icing Sugar-p
Icing Sugar
Corn Starch-p
Corn Starch
Eskal 2-p
Eskal 2
Carbamazepine-p
Carbamazepine

Figure 10

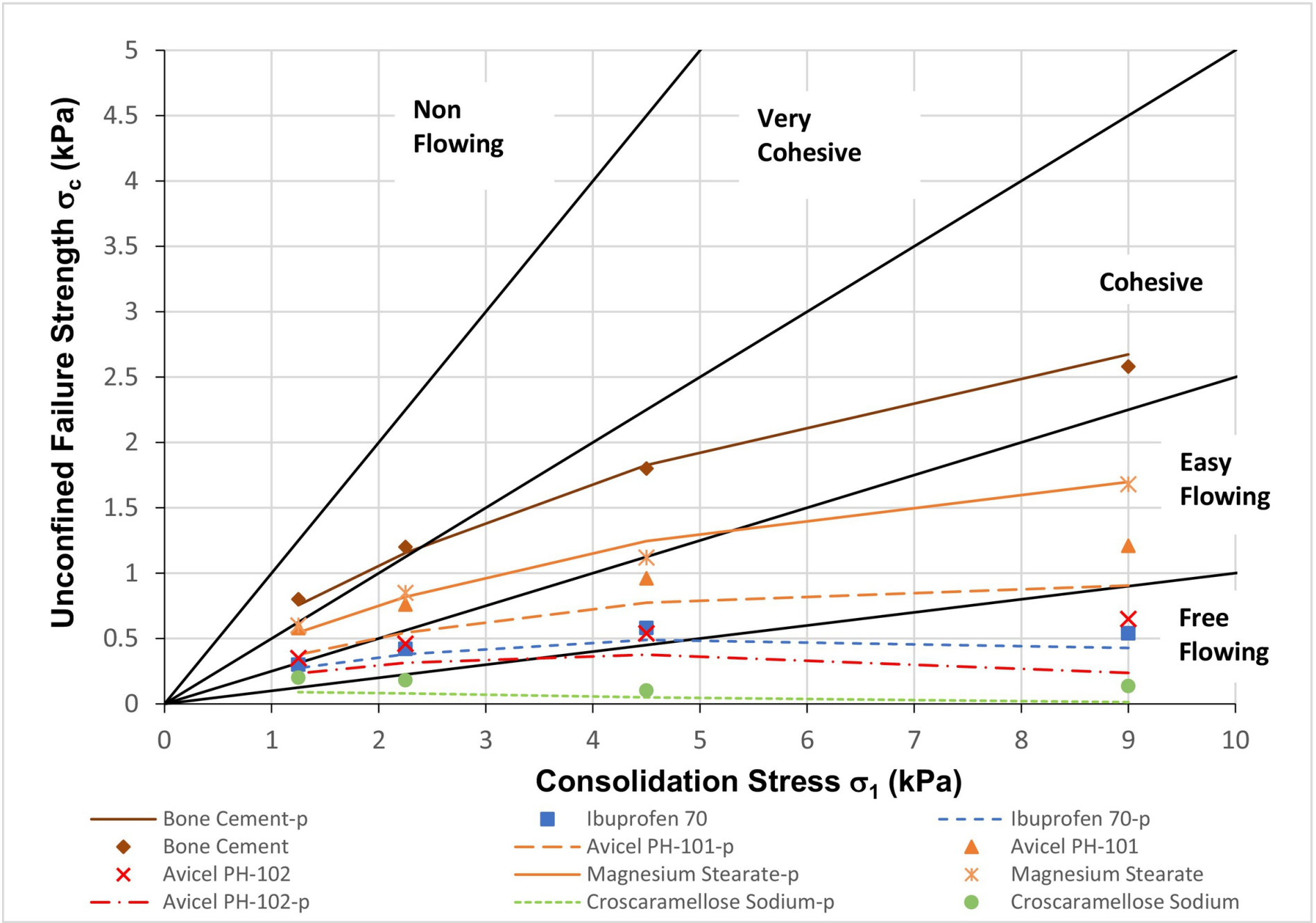
Unconfined Failure Strength σ_c (kPa)
Consolidation Stress σ_1 (kPa)
Non Flowing
Very Cohesive
Cohesive
Easy Flowing
Free Flowing
0
0.5
1
1.5
2
2.5
3
3.5
4
4.5
5
0
1
2
3
4
5
6
7
8
9
10
Bone Cement-p
Bone Cement
Avicel PH-102
Avicel PH-102-p
Ibuprofen 70
Avicel PH-101-p
Magnesium Stearate-p
Croscaramellose Sodium-p
Ibuprofen 70-p
Avicel PH-101
Magnesium Stearate
Croscaramellose Sodium

Figure 11

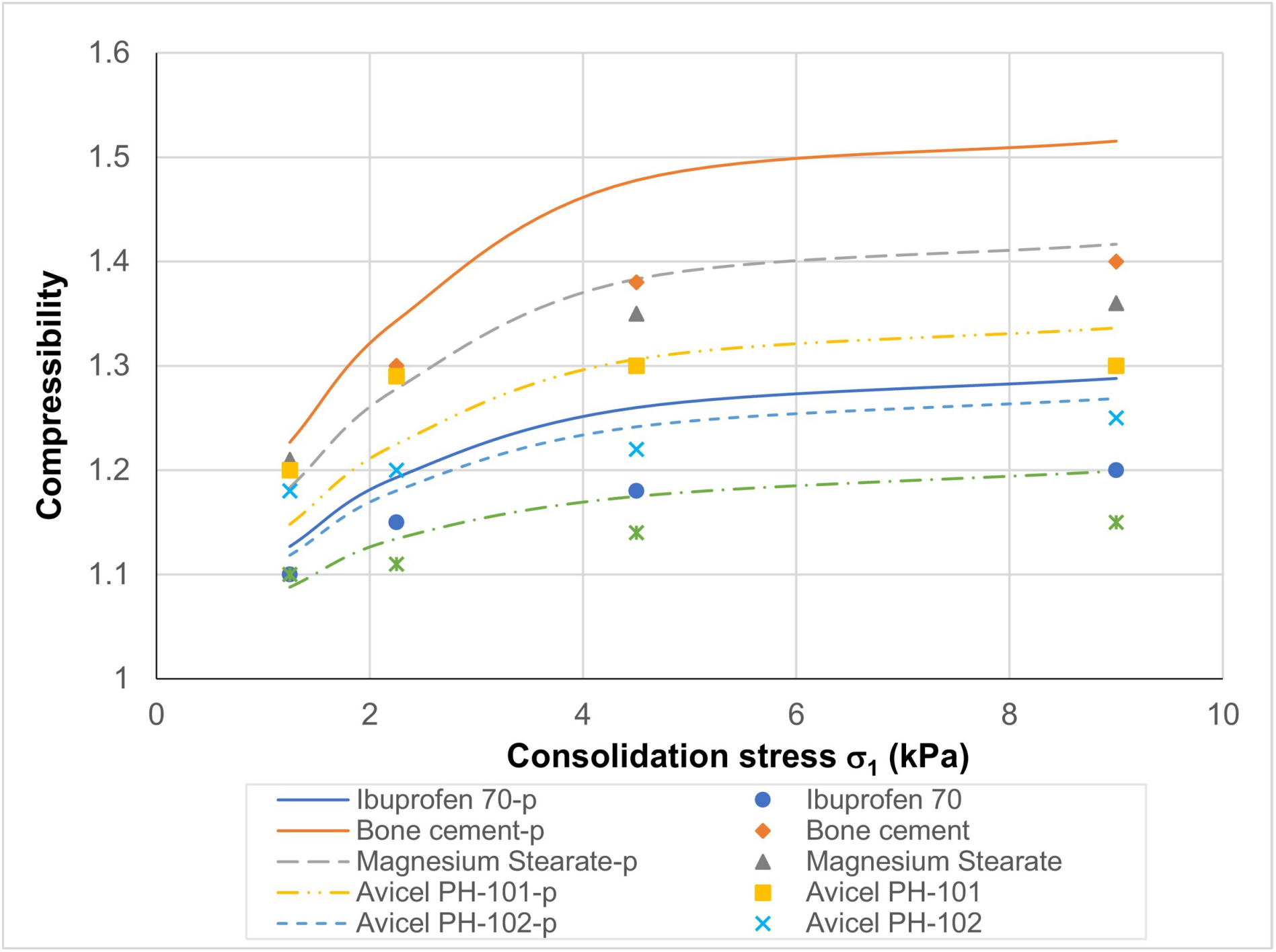
Compressibility
1.6
1.5
1.4
1.3
1.2
1.1
1
0
2
4
6
8
10
Consolidation stress σ1 (kPa)
Ibuprofen 70-p
Bone cement-p
Magnesium Stearate-p
Avicel PH-101-p
Avicel PH-102-p
Ibuprofen 70
Bone cement
Magnesium Stearate
Avicel PH-101
Avicel PH-102

Figure 12